PERIODICA POLYTECHNICA SER. MECH. ENG. VOL. 44, NO. 1, PP. 9–22 (2000)

LIFE EXPECTANCY CALCULATIONS OF TRANSIENT CHAOTIC BEHAVIOUR IN THE LORENZ MODEL

Gábor CSERNÁK and Gábor STÉPÁN

Department of Applied Mechanics
Technical University of Budapest
H–1521 Budapest, Hungary

Received: December 8, 1999

Abstract

In engineering practice, chaotic oscillations are often observed which disappear suddenly. This phenomenon is often referred to as transient chaos. The life expectancy of these oscillations varies stochastically. In this work, a method is presented for the simple estimation of the expected length of the chaotic behaviour. As an example, the Lorenz system is considered at some specific parameter values.

Keywords: Lorenz model, Hopf bifurcation, transient chaos, Poincaré map.

1. Introduction

There are several examples in engineering vibration problems where chaotic oscillations may occur. These oscillations appear much more often than engineers expect them. One reason for this is the fact that the chaotic oscillations often disappear suddenly – this phenomenon is referred to as transient chaos. This oscillation is usually considered by engineers as a regular motion since it may look like the conventional transient behaviour when a machine starts its operation. However, this transient behaviour cannot be characterised by conventional damping factors since the transient chaotic oscillation does not produce an exponential decay in amplitudes, it rather disappears unexpectedly. Actually, similar initial operation of a machine may produce very different time period of transient oscillations. The life expectancy of these oscillations – which can be an important parameter for the design work – varies stochastically, so the estimation of the duration of the transient motion needs extensive simulation work and statistical analysis. To avoid this we would like to develop a semi-analytical method, which can help us to give estimations quickly. The method is based on appropriate 1D maps, constructed by Poincaré sections.

We apply the proposed method in the so-called Lorenz model, because it is well-known and studied, and the equations are not complicated.

2. The Lorenz Model

2.1. Stability Analysis

For the analysis of the convection of heated fluid film, the equations introduced by Lorenz [1] are

$$\begin{aligned} \dot{x} &= -\sigma x + \sigma y, \\ \dot{y} &= \rho x - y - xz, \\ \dot{z} &= -\beta z + xy, \end{aligned} \tag{1}$$

where σ, β and ρ are positive parameters depending on the geometry and the physical properties of the fluid. This system of equations is the *Lorenz model*. We restrict ourselves to $\sigma = 10$ and $\beta = 8/3$, as Lorenz did.

For $\rho < 1$ the origin is the single fixed point: $P_0 = (0, 0, 0)$, while for $\rho > 1$ two more fixed points appear: $P_\pm = (\pm\sqrt{\beta(\rho-1)}, \pm\sqrt{\beta(\rho-1)}, \rho - 1)$.

The stability of the trivial solution of (1) can be investigated by means of the variational system:

$$\begin{pmatrix} \dot{x} \\ \dot{y} \\ \dot{z} \end{pmatrix} = \begin{pmatrix} -\sigma & \sigma & 0 \\ \rho & -1 & 0 \\ 0 & 0 & -\beta \end{pmatrix} \begin{pmatrix} x \\ y \\ z \end{pmatrix}.$$

The eigenvalues and the eigenvectors of the above matrix are:

$$\begin{aligned} \mu_{1,2} &= \frac{1}{2}\left[-(1+\sigma) \pm \sqrt{(1+\sigma)^2 + 4\sigma(\rho-1)}\right], \\ \mathbf{V}_{1,2} &= \left(1, \frac{1}{2\sigma}\left[-(1+\sigma) \pm \sqrt{(1+\sigma)^2 + 4\sigma(\rho-1)} + 2\sigma\right], 0\right), \\ \mu_3 &= -\beta, \\ \mathbf{V}_3 &= (0, 0, 1). \end{aligned} \tag{2}$$

Easy to see that if $\rho < 1$ all three eigenvalues are negative, while in the other case $\mu_1 > 0$, thus at $\rho = 1$ P_0 becomes unstable with a 2D invariant set spanned by $\mathbf{V}_2$ and $\mathbf{V}_3$.

Moving the origin of the coordinate system into the $P_\pm$ points we get the following equation:

$$\begin{pmatrix} \dot{x} \\ \dot{y} \\ \dot{z} \end{pmatrix} = \begin{pmatrix} -\sigma & \sigma & 0 \\ 1 & -1 & \mp\sqrt{\beta(\rho-1)} \\ \pm\sqrt{\beta(\rho-1)} & \pm\sqrt{\beta(\rho-1)} & -\beta \end{pmatrix} \begin{pmatrix} x \\ y \\ z \end{pmatrix} + \begin{pmatrix} 0 \\ -xz \\ xy \end{pmatrix} =$$

$$= A\mathbf{x} + \mathbf{f}(\mathbf{x}). \tag{3}$$

The characteristic equation of the matrix related to the linear part of this system:

$$\lambda^3 + (\beta + \sigma + 1)\lambda^2 + \beta(\rho + \sigma)\lambda + 2\sigma\beta(\rho - 1) = 0. \tag{4}$$

The Routh–Hurwitz criterion applied to coefficients results in the following condition of the exponential asymptotical stability of this solution:

$$\rho < \rho_{cr} = \frac{\sigma(\sigma+\beta+3)}{\sigma-\beta-1}.$$

Here $\sigma > \beta+1$ is assumed, which is fulfilled with the standard parameters. $\rho_{cr} \approx 24.74$ if $\beta = 8/3$ and $\sigma = 10$. It means that the losing of stability of R_0 passes off by means of a Pitchfork bifurcation, because at $\rho = 1$ the stable origin becomes unstable and two stable fixed points appear.

The characteristic equation at ρ_{cr}:

$$\lambda^3 + (\beta+\sigma+1)\lambda^2 + \frac{2\beta\sigma(\sigma+1)}{\sigma-\beta-1}\lambda + 2\sigma\beta\frac{\sigma^2+\sigma\beta+2\sigma+\beta+1}{\sigma-\beta-1} = 0. \quad (5)$$

As ρ exceeds ρ_{cr} the $P_\pm$ points become unstable. We may assume that at this point a Hopf bifurcation occurs. In the next section this suspicion is going to be proved.

2.2. Hopf Bifurcation Analysis

If P_+ and P_- lose stability by means of Hopf bifurcation, the complex conjugated roots ($\lambda_{1,2}$) of (4) must be pure imaginary at the critical value of parameter ρ, and the real part of the $\lambda' = \frac{d\lambda_{1,2}(\rho)}{d\rho}$ derivatives must not disappear at ρ_{cr} [2],[3].

Thus we can try to calculate these roots using the following assumption: $\lambda_{1,2} = \pm i\alpha$. Substituting these values into (5) we find that $\alpha = \sqrt{\frac{2\beta\sigma(\sigma+1)}{\sigma-\beta-1}}$ satisfies it. After dividing (5) by $(\lambda - i\alpha)(\lambda + i\alpha)$ we get the following system of eigenvalues:

$$\begin{aligned} \lambda_{1,2} &= \pm i\alpha = \pm i\sqrt{\frac{2\beta\sigma(\sigma+1)}{\sigma-\beta-1}}, \\ \lambda_3 &= -(\beta+1+\sigma). \end{aligned} \quad (6)$$

λ_3 is negative, thus there must be attractive manifolds in the neighbourhood of the $P_\pm$ points.

Now we have to prove that the real part of the λ' derivatives are not zero at the critical parameter. The simplest way to do it is to derive equation (4) taking into account that λ is function of ρ. After substituting $\lambda_{1,2}$ into the derivative of (4) the following equation results:

$$-3\alpha^2\lambda' \pm 2(\beta+1+\sigma)i\alpha\lambda' + \beta\sigma\lambda' \pm \beta i\alpha + \beta\frac{\sigma(\sigma+\beta+3)}{\sigma-\beta-1}\lambda' + 2\beta\sigma = 0.$$

Solving this simple equation we find that

$$\lambda'_{cr} = \frac{-(2\beta\sigma \pm \beta i\alpha)}{\pm 2(\beta+\sigma+1)i\alpha + \beta\frac{\sigma(\sigma+\beta+3)}{\sigma-\beta-1} + \beta\sigma - 3\alpha^2}.$$

With the standard parameters $\lambda'_{cr} \approx 0.0302225 \pm 0.1814503i$, thus the conditions of the Hopf bifurcation are fulfilled. It means that limit cycles exist around the $P_{\pm}$ points. The geometry and the stability properties of these cycles can be determined by the so-called Hopf bifurcation analysis. For applying this method we must calculate the eigenvectors of the A matrix in (3) at ρ_{cr}:

$$\mathbf{S}_{1,2} = \begin{pmatrix} 1 \\ 1 \pm \frac{\alpha}{\sigma} i \\ \frac{2b\beta\sigma + b\alpha^2 \pm (b\beta - 2b\sigma)\alpha i}{\sigma(\alpha^2+\beta^2)} \end{pmatrix}, \quad \mathbf{S}_3 = \begin{pmatrix} 1 \\ -\frac{\beta+1}{\sigma} \\ -\frac{\beta(\beta+1+\sigma)}{b\beta} \end{pmatrix}, \tag{7}$$

where $b = \sqrt{\beta \frac{\sigma^2+2\sigma+(\sigma+1)\beta+1}{\sigma-\beta-1}}$, α was defined above.

The plane spanned by the $\mathbf{S}_{1,2}$ vectors is tangent to the attractive central manifold at the origin, that is at P_+ or P_- depending on the chosen coordinate system. Using also the third eigenvector we can define a matrix:

$$T = (Re\mathbf{S}_1, Im\mathbf{S}_1, \mathbf{S}_3) = \begin{pmatrix} 1 & 0 & 1 \\ 1 & \frac{\alpha}{\sigma} & -\frac{\beta+1}{\sigma} \\ \frac{2b\beta\sigma + b\alpha^2}{\sigma(\alpha^2+\beta^2)} & \frac{(b\beta-2b\sigma)\alpha}{\sigma(\alpha^2+\beta^2)} & -\frac{\beta(\beta+1+\sigma)}{b\beta} \end{pmatrix} \tag{8}$$

and a new set of variables:

$$\begin{pmatrix} x \\ y \\ z \end{pmatrix} = T \begin{pmatrix} \xi_1 \\ \xi_2 \\ \xi_3 \end{pmatrix}.$$

With these new variables we get the so-called Poincaré normal form of equation (3):

$$\dot{\boldsymbol{\xi}} = T^{-1}AT\boldsymbol{\xi} + T^{-1}\mathbf{f}(T\boldsymbol{\xi}) = \begin{pmatrix} 0 & \alpha & 0 \\ -\alpha & 0 & 0 \\ 0 & 0 & \lambda_3 \end{pmatrix} \begin{pmatrix} \xi_1 \\ \xi_2 \\ \xi_3 \end{pmatrix} +$$

$$+ \begin{pmatrix} \sum\limits_{\substack{j+k+l=2 \\ j,k,l \geq 0}} m_{jkl} \xi_1^j \xi_2^k \xi_3^l \\ \sum\limits_{\substack{j+k+l=2 \\ j,k,l \geq 0}} n_{jkl} \xi_1^j \xi_2^k \xi_3^l \\ \sum\limits_{\substack{j+k+l=2 \\ j,k,l \geq 0}} o_{jkl} \xi_1^j \xi_2^k \xi_3^l \end{pmatrix}, \tag{9}$$

To be able to calculate the radius of the limit cycle we must separate the third variable ξ_3. This can be done using the center manifold theorem [4]. It means that we can approximate ξ_3 with the following expression:

$$\xi_3 = h_1\xi_1^2 + h_2\xi_1\xi_2 + h_3\xi_2^2.$$

The derivative of this formula:

$$\dot{\xi}_3 = 2h_1\xi_1\dot{\xi}_1 + h_2(\xi_1\dot{\xi}_2 + \xi_2\dot{\xi}_1) + 2h_3\xi_2\dot{\xi}_2.$$

Taking into account that $\dot{\xi}_1 \approx \alpha\xi_2$ and $\dot{\xi}_2 \approx -\alpha\xi_1$ we get that

$$\dot{\xi}_3 = -h_2\alpha\xi_1^2 + h_2\alpha\xi_2^2 + (2h_1 - 2h_3)\alpha\xi_1\xi_2.$$

Substituting the expression of ξ_3 into (9) $\dot{\xi}_3$ can be expressed in another way. Comparing the corresponding terms of the two expressions and neglect the higher order ones, the h_i coefficients can be calculated:

$$\begin{aligned} h_1 &= \frac{\lambda_3\alpha(T_{32}^2 + T_{22}^2) - (\lambda_3^2 + 2\alpha^2)(T_{32}T_{31} + T_{22})}{\det(T)(\lambda_3(\lambda_3^2 + 2\alpha^2) + 2\lambda_3\alpha^2)}, \\ h_3 &= \frac{2\alpha^2 h_1 \det(T) - (T_{32}^2 + T_{22}^2)\alpha}{\det(T)(\lambda_3^2 + 2\alpha^2)}, \\ h_2 &= \frac{\lambda_3 h_3}{\alpha}. \end{aligned}$$

Here the elements of the T matrix – whose determinant is $\det(T)$ – are denoted by T_{ij}.

Thus the first two rows of (9) can be separated:

$$\begin{pmatrix} \dot{\xi}_1 \\ \dot{\xi}_2 \\ \dot{\xi}_3 \end{pmatrix} = \begin{pmatrix} 0 & \alpha & 0 \\ -\alpha & 0 & 0 \\ 0 & 0 & \lambda_3 \end{pmatrix} \begin{pmatrix} \xi_1 \\ \xi_2 \\ \xi_3 \end{pmatrix} + \begin{pmatrix} \sum\limits_{\substack{j+k=3 \\ j,k>0}} a_{jk} & \xi_1^j \xi_2^k + \dots \\ \sum\limits_{\substack{j+k=3 \\ j,k>0}} b_{jk} & \xi_1^j \xi_2^k + \dots \\ \dots & \end{pmatrix}, \quad (10)$$

where the coefficients are the following:

$$\begin{aligned} a_{20} &= -\frac{T_{32}T_{31} + T_{22}}{\det(T)}, \quad a_{02} = 0, \quad a_{11} = -\frac{T_{32}^2 + T_{22}^2}{\det(T)}, \quad a_{12} = a_1h_3 + a_2h_2, \\ a_{21} &= a_1h_2 + a_2h_1, \quad a_{30} = a_1h_1, \quad a_{03} = a_2h_3, \end{aligned}$$

$$\begin{aligned} b_{20} &= \frac{T_{31}(T_{31} - T_{33}) + (1 - T_{23})}{\det(T)}, \quad b_{02} = 0, \quad b_{11} = b_2, \quad b_{12} = b_1h_3 + b_2h_2, \\ b_{21} &= b_1h_2 + b_2h_1, \quad b_{30} = b_1h_1, \quad b_{03} = b_2h_3, \end{aligned}$$

where

$$\begin{aligned} a_1 &= \frac{-T_{32}(T_{33} + T_{31}) + T_{22}(T_{23} + T_{21})}{\det(T)}, \quad a_2 = -\frac{T_{32}^2 + T_{22}^2}{\det(T)} \\ b_1 &= \frac{T_{31}^2 - T_{33}^2 + 1 - T_{23}^2}{\det(T)}, \quad b_2 = \frac{T_{32}(T_{31} - T_{33}) + T_{22}(1 - T_{23})}{\det(T)}. \end{aligned}$$

These coefficients are needed for the calculation of the parameter

$$\delta = \frac{1}{8}\left\{\frac{1}{\alpha}\Big[(a_{20}+a_{02})(-a_{11}+b_{20}-b_{02})+(b_{20}+b_{02})(a_{20}-a_{02}+b_{11})\Big]+\right.$$

$$\left.+(3a_{30}+a_{12}+b_{21}+3b_{03})\right\}.$$

With the standard parameters $\delta \approx 0.0038669$. As shown in [3], the positiveness of δ proves the existence of a subcritical Hopf bifurcation, that is unstable periodic solutions exist around the $P_{\pm}$ points. The amplitude r of this periodic motion can be given in the following simple form (see [3]):

$$r = \sqrt{-\frac{Re\lambda'_{cr}}{\delta}(\rho-\rho_{cr})}.$$

Now the curve of the limit cycle is given by

$$\begin{pmatrix}\xi_1\\ \xi_2\\ \xi_3\end{pmatrix} = \begin{pmatrix} r & \sin(\alpha t)\\ r & \cos(\alpha t)\\ & 0\end{pmatrix},$$

but these formulae are written in the transformed coordinate system, so we have to transform them back into the original one:

$$\begin{pmatrix}x\\ y\\ z\end{pmatrix} = T\begin{pmatrix}\xi_1\\ \xi_2\\ \xi_3\end{pmatrix} =$$

$$= \begin{pmatrix} r & \sin(\alpha t)+x_0\\ r & \sin(\alpha t)+r & \frac{\alpha}{\sigma}\cos(\alpha t)+y_0\\ r & \frac{2b\beta\sigma+b\alpha^2}{\sigma(\alpha^2+\beta^2)}\sin(\alpha t)+r & \frac{b\beta-2b\sigma}{\sigma(\alpha^2+\beta^2)}\cos(\alpha t)+z_0\end{pmatrix}.$$

Here (x_0, y_0, z_0) are the coordinates of the P_+ or the P_- points. Obviously, there may be difference between the above calculated curve and the real limit cycle, because some higher order terms were neglected. In the first picture the phase space of the Lorenz model can be seen, with a cylinder drawn onto the limit cycle around P_+. This cylinder is parallel to the attracting eigenvector of A, thus if a trajectory starts from the inside of it, the motion will damp out, while in the other case the trajectory tends to the center manifold, but moves away from the fixed point.

As numerical investigations show [5, 6], in the $1 < \rho < 13.926$ range there are no limit cycles, because as we decrease ρ from ρ_{cr} the limit cycles expand, and at $\rho = 13.926$ they touch the origin and a homoclinic bifurcation occurs. In this parameter range the trajectories begin to tend to one of the fixed points immediately. On the other hand at $\rho \approx 24.06$ the so-called Lorenz attractor evolves, and for $\rho > 24.06$ the trajectories tend to the fixed points only with 0 possibility. But

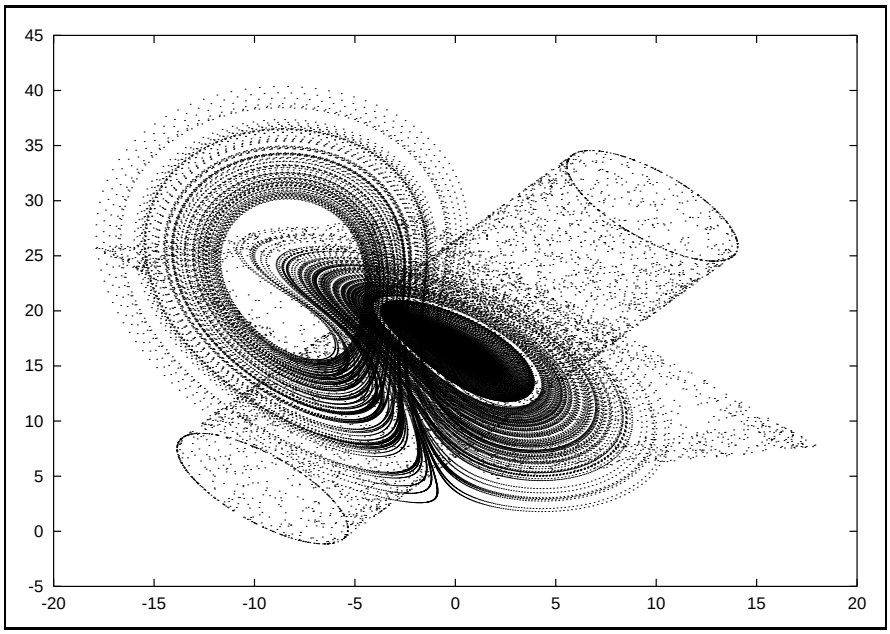

Fig. 1. The phase-space of the Lorenz system

in the $13.926 \lesssim \rho \lesssim 24.06$ range transient chaotic motion occurs. It means that after some chaotic switches between the circulation around P_+ and the circulation around P_-, the trajectory may jump inside one or another limit cycle, and tends to one of the stable fixed points. In the next section we are going to try to estimate the life expectancy of this transient oscillation.

3. Estimation of the Duration of the Transient Chaotic Behaviour

3.1. Reduction of the Complexity

The complexity of the system can be reduced if we switch to the examination of a two-dimensional Poincaré map. The Σ Poincaré surface is the $z = \rho - 1$ plane, which contains the $P_\pm$ points. The map is defined by the intersection points which we get as the trajectory of a solution intersects the Σ plane from the upward direction. In the next figure these points are presented between the fixed points, while the other two branches belong to the intersections from downward.

As it was already mentioned, if $\rho > 1$ the origin is a saddle point with a 2D invariant set. The intersection of Σ and this invariant set divides the Poincaré plane into two parts: the P_+ and P_- half-plane. The intersection curve is approximated with a line in *Fig. 2*.

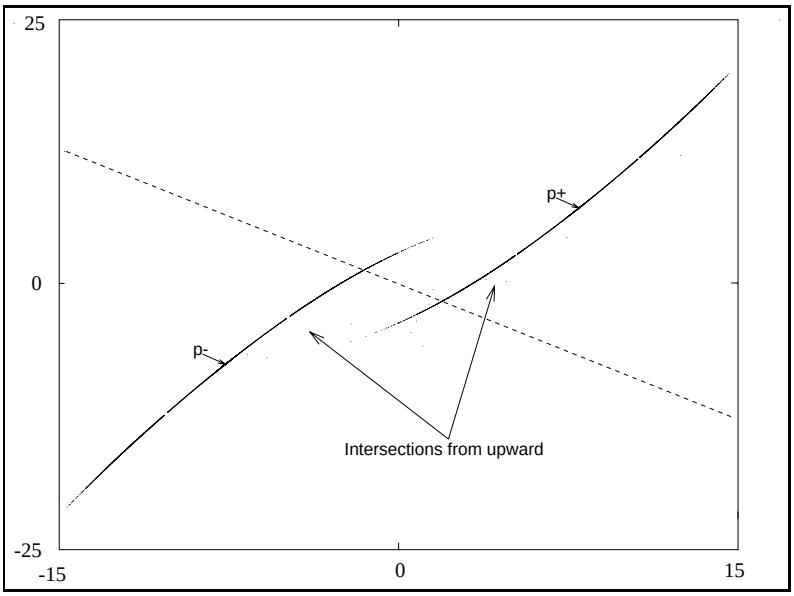

Fig. 2. The 2D Poincaré map

If we have a 2D Poincaré map, we can reduce it to a one-dimensional one by the following procedure. We project the points of the 2D map – which belong to intersections from *upward* – on the $P_+ - P_-$ line perpendicularly, then we measure the distance of the obtained points from one of the fixed points. If the last intersection from the *downward* direction took place on the P_+ half-plane, we measure the distance from P_+, while in the other case from P_-. Denoting the nth distance by M_n, and plotting the successive pairs (M_n, M_{n+1}) we get a sharply peaked Λ shaped curve. In *Fig. 3* the result of simulations starting from 15 different initial points is presented at $\rho = 23$.

The construction makes possible to distinguish the points which we get when the trajectory only oscillates around a fixed point – these are on the left branch of the graph – from the points which evolve after a jump to the other fixed point – the right branch belongs to these points.

The E point on the outside right belongs to a trajectory starting from the neighborhood of the origin, while the unstable fixed point on the left (F_s) indicates the unstable limit cycles around the stable fixed points of the original system. The method treats these fixed points together, their image is in the origin. Easy to see, that a trajectory starting from the section between the origin and F_s tends to the origin, because the graph of the map is below the diagonal line.

There is another fixed point on the right as well (F_b). It indicates that there may exist an unstable solution when the trajectory oscillates periodically between P_+ and P_-.

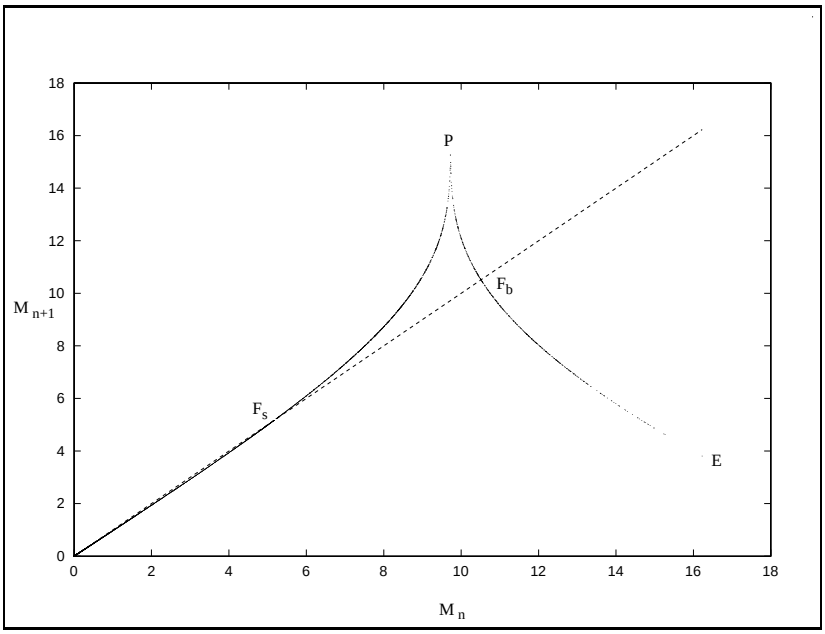

Fig. 3. The 1D map

3.2. Estimation Method

To make estimations on the base of the 1D map we must find a simple formula to express it explicitly. If the formula is not simple enough, the "mean kickout number" – the average number of intersections before the trajectory jumps in an attracting set – cannot be determined.

Piecewise linear maps may be suitable for trying to make analytical estimations. First we fitted a section to the smaller fixed point (F_s) and the maximum of the curve (P), and another section to K_b and P. K_b is that point on the right branch of the curve which has the same 'M_{n+1}' coordinate as F_s has. See *Fig. 4.*

We assumed that the maximum of the peak (P) equals the 'M_n' coordinate of E, although the tangent of the curve increases very quickly in the neighbourhood of P.

Let us denote the tangent of the $\overline{F_s P}$ section by t_1, the absolute value of the tangent of $\overline{P K_b}$ by t_2, the $\overline{K_b E}$ section by I_1 and the section between the origin and F_s by I_0. In the following I_0 and I_1 will also denote the length of the projections of these sections on the M_n axis.

Using an interpolation method or a simple data processing program these data can easily be measured, because the shape of the graph evolves quickly after few simulations.

The sequence of the ideas is the following: the trajectory can jump into the

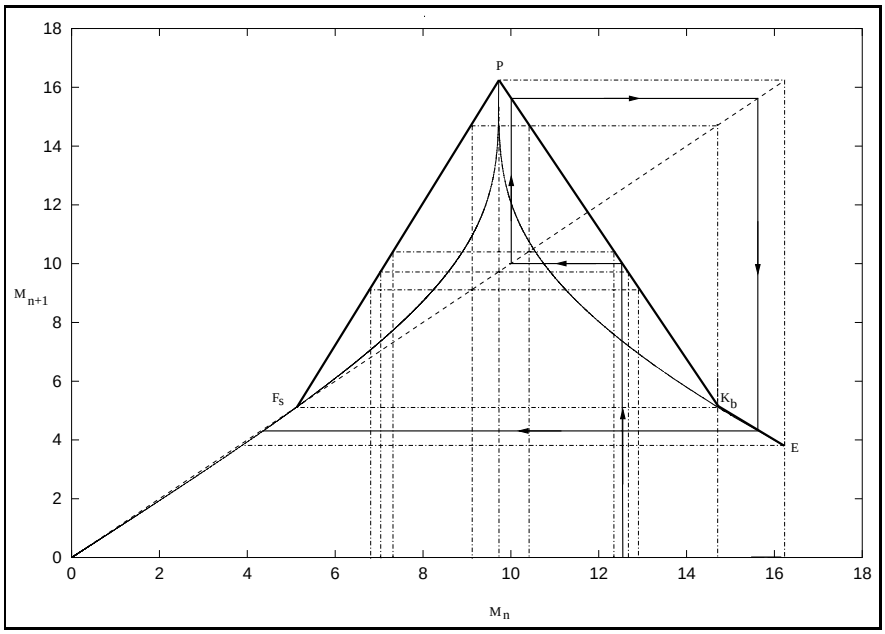

Fig. 4. The first approximation of the curve

attracting domain (I_0) only from I_1. Thus if we want to know, how many iteration steps are needed to reach I_0, it is obvious to calculate the pre-images of I_1. There are two intervals from which 2 steps lead to I_0, the length of them is I_1/t_1 and I_1/t_2. Easy to see that 2^{n-1} intervals belong to n steps. The length of the intervals can be represented in a tree-structure:

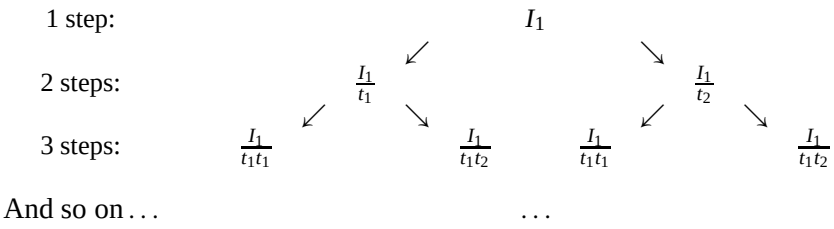

Denoting the joint length of the intervals from which n steps lead to I_0 by s_n, we get that

$$S = \sum_0^\infty s_n = I_0 + I_1 + \frac{S}{t_1} + \frac{S}{t_2} = I_0 + I_1 \frac{t_1 t_2}{t_1 t_2 - t_1 - t_2}.$$

This quantity is needed to estimate the mean kickout number:

$$N = \frac{\sum_0^\infty n s_n}{\sum_0^\infty s_n}. \tag{11}$$

The numerator of (11) can be calculated with the above introduced recursive method. The weighted sum forms a tree-structure:

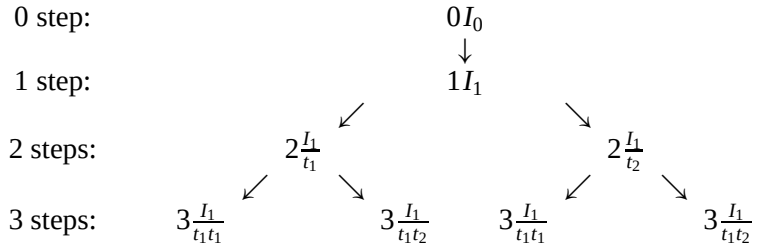

And so on . . . . . .

Using simple considerations we get that

$$A_1 = \sum_0^\infty n s_n = I_1 + \frac{A_1 + S}{t_1} + \frac{A_1 + S}{t_2} = I_1 \frac{(t_1 t_2)^2}{(t_1 t_2 - t_1 - t_2)^2},$$

thus

$$N_1 = \frac{A_1}{S} = I_1 \frac{(t_1 t_2)^2}{I_0 (t_1 t_2 - t_1 - t_2)^2 + I_1 t_1 t_2 (t_1 t_2 - t_1 - t_2)}.$$

Unfortunately N_1 differs considerably from the result of simulations, therefore we tried to apply a better approximation. See *Fig. 5*.

As it can be seen in the figure, there are two breakpoints on the sections on both sides: F_b, the bigger fix point, and M, the point on the other branch, which has the same M_{n+1} coordinate as F_b has.

Let us denote the tangent of $\overline{F_s M}$ by t_1, the tangent of $\overline{MP}$ by t_2, the absolute value of the tangent of $\overline{PF_b}$ by t_3, and the absolute value of the tangent of $\overline{F_b K_b}$ by t_4!

The $S = \sum_0^\infty s_n$ sum can also be calculated with considerations based on a tree-structure:

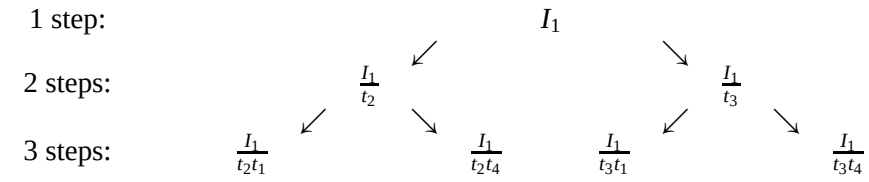

And so on . . . . . .

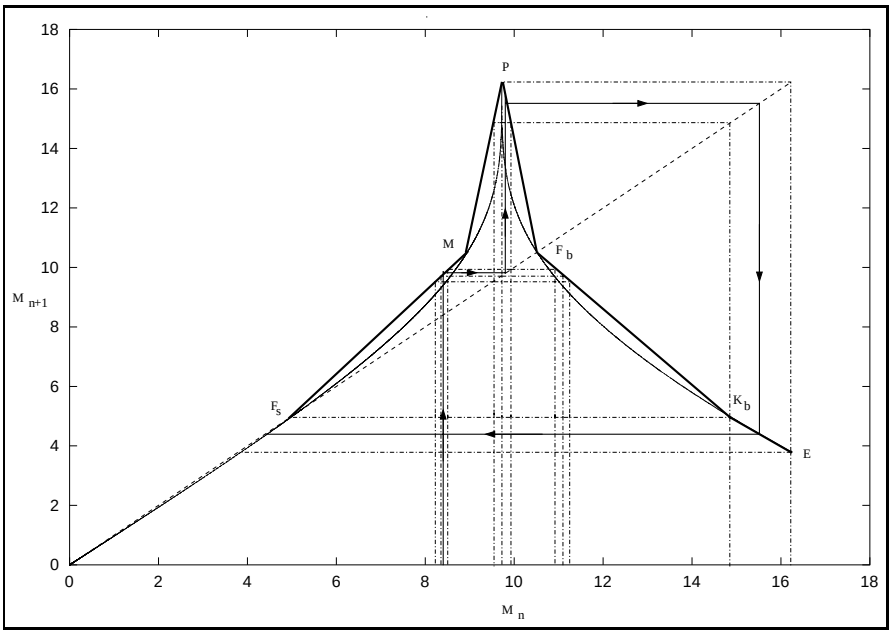

Fig. 5. The second approximation

This tree is more complicated than in the former case; after rather long calculations we get:

$$S = \sum_0^\infty s_n = I_0 + I_1 t_4 \frac{(t_1-1)(t_2t_3+t_2+t_3)+t_2+t_3}{(t_1-1)(t_2t_3t_4-t_2-t_3)-t_2-t_3}$$

and

$$A_2 = \sum_0^\infty n s_n = \frac{I_1(1+(2+\frac{3}{t_1-1})(\frac{1}{t_2}+\frac{1}{t_3}))+\frac{S-I_0}{t_4}(\frac{1}{t_2}+\frac{1}{t_3})(2+\frac{3}{t_1-1})}{Z*S} + \frac{K(\frac{1}{t_1-1}+\frac{t_2}{t_3(t_1-1)})}{Z*S},$$

where

$$Z = \frac{t_4-(\frac{1}{t_2}+\frac{1}{t_3})\frac{t_1}{t_1-1}}{t_4},$$

$$K = \frac{I_1t_4+S-I_0}{t_2t_4(t_1-1)}.$$

These formulae are rather messy, therefore we verified them by simulation of the piecewise linear map. The results were very close to the calculated values.

In *Fig. 6* the results of the two approximations (N_1 and $N_2 = \frac{A_2}{S}$) and an extended simulation work are represented. Here the mean kickout numbers can be seen as functions of the parameter ρ.

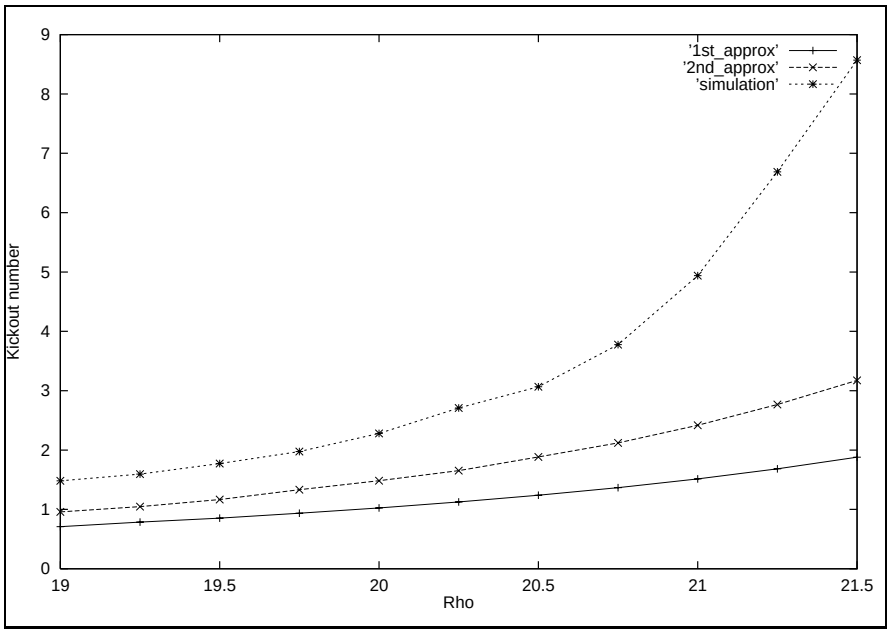

Fig. 6. Kickout numbers in the Lorenz model

As it can be seen, the second approximation provided much better results than the first one, but unfortunately at larger ρ parameters the curve which belongs to the simulations moves away from the curves constructed using the above introduced method.

3.3. Possibilities to Improve the Method

– During the simulations 8000 trajectories were investigated, starting with uniform probability density from a circle around the z axis, whose z coordinate was a bit less than $\rho - 1$ – so it was below the Σ plane –, and its radius was $2\sqrt{\beta(\rho - 1)}$. In the approximation methods we assumed that the initial points were distributed uniformly below the graph. Probably the results would be better, if we could find what kind of set of initial conditions corresponds to this assumption.

– The most obvious way to improve the efficiency of the method is to increase the number of the approximating sections. Unfortunately, it is very likely that the

appropriate formulae are hard to obtain, but it also can happen that choosing the endpoints properly, the difficulties disappear, and we can trace the equations back to the above obtained ones.

– Probably approximating of the curve in *Fig. 3* with quadratic or other functions, the estimation method would provide better results, but in this case it also seems to be hard to obtain the appropriate formulae.

Our future goal is to apply the above mentioned possibilities.

Acknowledgement

This research was supported by the Hungarian National Science Foundation under grant no. OTKA T030762/99, the Ministry of Education and Culture grant no. MKM FKFP 0380/97, and the EU COST Action P4.

References

[1] LORENZ, E. H.: Deterministic Nonperiodic Flow, *J. of Atmospheric Sci.* Vol. 20, 130, 1963.
[2] GUCKENHEIMER, J. – HOLMES, P.: Nonlinear Oscillations, Dynamical Systems and Bifurcation of Vector Fields, Springer, New York, 1983.
[3] HASSARD, B. D. – KAZARINOFF, Y. H. – WAN, Y. H.: Theory and Applications of Hopf Bifurcation, London Mathematical Society Lecture Notes Series 41, Cambridge, 1981.
[4] WIGGINS, S.: Introduction to Applied Nonlinear Dynamical Systems and Chaos, Texts in Applied Mathematics 2, Springer, New York, 1990
[5] YORKE, J. A. – YORKE, E. D.: Metastable Chaos: The Transition to Sustained Chaotic Behavior in the Lorenz Model, *Journal of Statistical Physics*, Vol. 21, No. 3, 1979.
[6] STROGATZ, S. H.: Nonlinear Dynamics and Chaos, Addison-Wesley Publishing Company, 1994.